PROCEEDINGS REPRINT
SPIE—The International Society for Optical Engineering

Reprinted from

Grazing Incidence and Multilayer X-Ray Optical Systems

27–29 July 1997
San Diego, California

Volume 3113

Calibration of the AXAF observatory: Overview

M. C. Weisskopf[a] and S. L. O'Dell[b]

[a]NASA Marshall Space Flight Center, ES01
Huntsville, AL 35812 USA

[b]NASA Marshall Space Flight Center, ES84
Huntsville, AL 35812 USA

ABSTRACT

The Advanced X-ray Astrophysics Facility (AXAF) will soon begin its exploration of the x-ray universe, providing unprecedented angular and spectral resolution. Also unprecedented is the ambitious goal of calibrating the AXAF observatory to an accuracy of a few percent. Toward this end, AXAF science and engineering teams undertook an extensive calibration program at component, subsystem, and system levels. This paper is an overview of the system-level calibration activities, conducted over the past year at the Marshall Space Flight Center (MSFC) X-Ray Calibration Facility (XRCF).

Keywords: x rays, calibration, grazing-incidence optics, gratings, detectors, x-ray imaging, x-ray spectroscopy.

1. INTRODUCTION

In late 1998, the Advanced X-ray Astrophysics Facility (AXAF) will join the Hubble Space Telescope (HST) and the Compton Gamma-Ray Observatory (CGRO), as one of NASA's "Great Observatories". With unique capabilities for sub-arcsecond imaging and spectrometric imaging, as well as high-resolution dispersive spectroscopy, the AXAF will enable x-ray (0.1–10 keV) observations of many categories of astronomical objects, in order to address a broad range of astrophysical questions.

Previously, we presented overviews of the AXAF flight-system design and expected performance[1] and of the development of the AXAF optics and science instruments.[2] Here (see also Ref. 3), we give an overview of the calibration of the AXAF observatory at the NASA Marshall Space Flight Center (MSFC) X-Ray Calibration Facility (XRCF). First (§2.), we describe the x-ray calibration instrumentation; next (§3.), the calibration activities at the XRCF; and finally (§4.), a few key preliminary results. Several papers in these and other* Proceedings describe calibration activities and preliminary results for specific subsystems of the AXAF observatory. In addition, Appendix A lists several web sites for accessing more information about AXAF and its calibration. The calibration program at the XRCF was quite successful: Not only did it accumulate data essential to the calibration, but it also provided an end-to-end test and verification of the flight AXAF observatory system.

2. X-RAY CALIBRATION INSTRUMENTATION

The X-Ray Calibration Facility (XRCF), operated by MSFC's System Analysis and Integration Laboratory (SAIL), provides unique capabilities for testing and calibrating the AXAF observatory and related activities. The facility includes a 518-m guide tube, separating the x-ray-source building from the Instrument Chamber (IC). With a usable volume of 18-m length by 6-m diameter, the Instrument Chamber provides a controlled thermal–vacuum environment sufficiently large to accommodate any payload that will fit into the Space Shuttle Orbiter's bay.

In this section, we describe x-ray instrumentation, both ground-support and flight, used during AXAF testing and calibration activities at the XRCF. Figure 1 indicates the various x-ray components involved in the calibration — namely, the source system (§2.1.), the monitor detectors (§2.2.), the x-ray optics (§2.3.), the transmission gratings (§2.4.), and the focal-plane detectors (§2.5.).

Other author information: (Send correspondence to S.L.O.)
S.L.O.: odell@cosmos.msfc.nasa.gov; Voice: 205-544-7708; Fax: 205-544-7754.
M.C.W.: martin@cosmos.msfc.nasa.gov; Voice: 205-544-7740; Fax: 205-544-7754.
EUV, X-Ray, and Gamma-Ray Instrumentation for Astronomy, O. H. Siegmund and M. A. Gummin, eds., *Proc. SPIE* **3114**, 1997.

SPIE Vol. 3113 • 0277-786X/97/$10.00

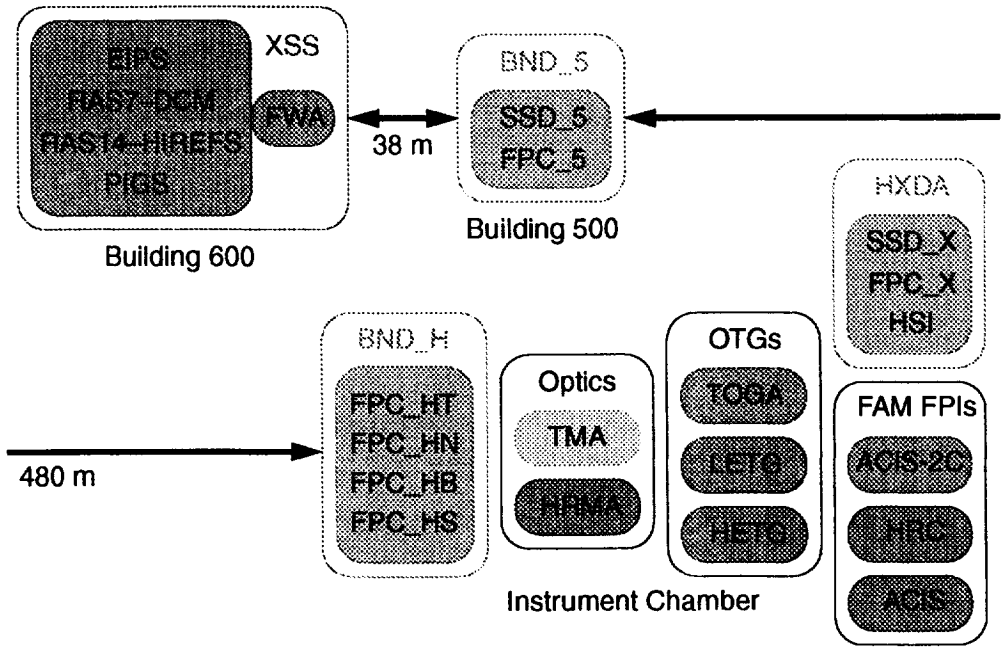

Figure 1. Configurations of x-ray sources, monitor detectors, x-ray optics, transmission gratings, and focal-plane detectors during calibration of the AXAF observatory at the MSFC X-Ray Calibration Facility (XRCF).

2.1. X-ray Source System (XSS)

The X-ray Source System[4] (XSS) comprises a conventional electron-impact source, two monochromators, a Penning source, and transmission filters. MSFC SAIL integrated the XSS; AXAF Project Science characterized the XSS prior to AXAF calibration. In addition to the x-ray sources of the XSS, the AXAF optics and both focal-plane instruments employ flight, radioactive calibration sources to ensure an accurate ground-to-orbit transfer of the AXAF flux scale.[5]

2.1.1. Electron-Impact Point Source (EIPS)

MSFC's System Analysis and Integration Laboratory (SAIL) developed the Electron-Impact Point Source (EIPS), which produces electron-induced fluorescence lines and bremsstrahlung in its fixed, oil-cooled anode. A large number of interchangeable, conical, anode targets provide atomic K and L lines over the AXAF energy range (0.1–10 kev).

2.1.2. Double-Crystal Monochromator (DCM)

The National Institute of Standards and Technology (NIST) fabricated the dual-pentagonal-turret Double-Crystal Monochromator (DCM). The AXAF calibration employed Thallium Acid Phthalate (TAP001), germanium (Ge111), and abraded silicon (aSi400) crystals to span the respective energy ranges of 0.7–2.3, 2.1–9.0, and 6–12 keV. Rigaku manufactured the Rotating Anode Source (RAS) used with the DCM.

2.1.3. Reflection-grating monochromator

Hettrick Scientific fabricated the reflection-grating monochromator, named HIgh-Resolution Erect Field Spectrometer (HIREFS). The AXAF calibration employed 3 of the HIREFS' 4 selectable gratings to span the energy ranges of 0.12–0.40, 0.30–1.2, and 0.9–2.0 keV. Rigaku manufactured the Rotating Anode Source (RAS) used with the HIREFS.

2.1.4. Penning Ionization Gas-discharge Source (PIGS)

The Smithsonian Astrophysical Observatory (SAO) Mission Support Team (MST) provided the Penning Ionization Gas-discharge Source (PIGS); MSFC SAIL refurbished the PIGS during the calibration. The PIGS produces narrow, soft-x-ray L lines of ionized aluminum and argon, for calibrating spectral resolution of the AXAF gratings in the energy range 0.07–0.25 keV (wavelengths 170–50 Å).

2.1.5. Filter-Wheel Assembly (FWA)

MSFC's System Analysis and Integration Laboratory (SAIL) developed a dual-wheel Filter-Wheel Assembly (FWA), which holds assorted x-ray transmission filters, pin holes, occulting bars, and open (unobstructed) apertures. Nominally, the filters provide 2, 4, or (when used in combination) 6 mean-free-path attenuation at the characteristic lines produced in EIPS anode targets.

2.2. Beam-Normalization Detectors (BNDs)

The Smithsonian Astrophysical Observatory (SAO) Mission Support Team (MST) provided the HRMA X-ray Detection System[6] (HXDS), which comprises Beam-Normalization Detectors (BNDs) to monitor the x-ray source and (non-flight) focal-plane detectors (§2.5) to characterize x-ray optics (§2.3) and gratings (§2.4). Of the 6 BNDs, 1 (§2.2.1) is a Solid-State Detector (SSD) and the other 5 (§2.2.2) are Flow Proportional Counters (FPCs).

2.2.1. Solid-State Detector (SSD)

The BND SSD ("SSD_5"), residing approximately 38 m from the XSS (§2.1), is a liquid-nitrogen-cooled, high-purity-germanium (hpGe) detector,[7] with a resolving power $(E/(\Delta E))$ of $8.0\sqrt{(E/(1\,\mathrm{keV}))}/\sqrt{((1\,\mathrm{keV})/E)+0.15}$. In front of the detector's 6-mm-diameter active area, lies an aperture wheel, holding circular apertures up to 5-mm diameter and a radioactive calibration source. Prior to the AXAF calibration, SAO and Physikalisch–Technische Bundesanstalt (PTB) calibrated[8] this SSD at the Berliner Elektronenspeicherring-Gesellschaft für Synchrotronstrahlung (BESSY).

2.2.2. Flow Proportional Counters (FPCs)

One BND FPC ("FPC_5") lies slightly in front of the BND SSD (SSD_5), about 38 m from the XSS (§2.1). This BND, FPC_5, has an aperture slide, with aperture diameters of 1, 4, 12, and 36 mm; it is mounted on a 2-degree-of-freedom stage, for mapping the x-ray beam. Four BND FPCs ("FPC_H") reside just in front of the x-ray optic, about 526 m from the source; one of these is mounted on a 2-degree-of-freedom stage for mapping the x-ray beam near the optic's entrance aperture. All HXDS FPCs are essentially identical and have a spectral resolving power of approximately $2.6\sqrt{((1\,\mathrm{keV})/E)}$. SAO and PTB will calibrate the absolute efficiencies of the FPCs at BESSY.

2.3. X-ray optics

Calibration activities at the XRCF involved not only the flight optic (§2.3.1), the High-Resolution Mirror Assembly (HRMA), but a non-flight optic (§2.3.2), the Technology Mirror Assembly (TMA). Use of the TMA allowed a realistic rehearsal of the calibration, prior to arrival of the (flight) HRMA.

2.3.1. High-Resolution Mirror Assembly (HRMA)

The Eastman Kodak Company (EKC) aligned and assembled the HRMA; Hughes Danbury Optical Systems (HDOS) figured and polished its Zerodur mirrors; and Optical Coatings Laboratories Inc. (OCLI) sputter-coated the optical surfaces with iridium. With 4 Wolter-1 paraboloid–hyperboloid mirror pairs (segment lengths of 0.83 m and diameters of 0.63, 0.85, 0.97, and 1.2 m), the HRMA[2,9] provides both high-resolution (sub-arcsecond) imaging and a large (1140 cm^2) geometric area. With a focal length of 10 m, the HRMA focal-plane plate scale is about 50-μm/arcsec. EKC provided HRMA ground-support equipment, including actuators to yaw and pitch the HRMA for off-axis measurements and a 16-shutter assembly to isolate specific HRMA mirror-shell quadrants.

Complementing the HRMA calibration at the XRCF, SAO developed accurate finite-element and ray-trace models, incorporating extensive data from metrology collected at HDOS and at EKC, to simulate the performance[9–11] of the HRMA. Furthermore, using the National Synchrotron Light Source (NSLS) at Brookhaven National Laboratory (BNL), SAO and Los Alamos National Laboratory (LANL) are determining[12–14] the optical constants of iridium coatings deposited on witness flats during qualification runs and coating of the AXAF mirrors at OCLI. An important objective of the calibration is to understand the measured HRMA effective area,[15] in terms of the simulations (e.g., §4.3.3).

2.3.2. Technology Mirror Assembly (TMA)

The TMA is a gold-coated 60%-scale model of the smallest of the AXAF's 4 mirror shells. Fabricated and tested a decade earlier, as a demonstration of technologies to be used in producing the mirrors for AXAF, the TMA served as a surrogate optic during calibration rehearsals, prior to arrival of the (flight) HRMA.

2.4. Objective transmission gratings

Located immediately behind an optic, objective transmission gratings (OTGs) disperse the convergent beam, to form high-resolution spectra on the focal plane. The AXAF observatory has 2 sets of OTGs — (§2.4.1) the Low-Energy Transmission Grating (LETG) and (§2.4.2) the High-Energy Transmission Grating (HETG) — either of which may be inserted into the x-ray path behind the HRMA. Because the flight OTGs (LETG and HETG) are matched to the HRMA's geometry, the custom-built (§2.4.3) TMA Objective Grating Assembly (TOGA), using flight-type gratings from the LETG and the HETG, allowed a realistic rehearsal of high-resolution-spectroscopy data collection and analysis with the TMA (§2.3.2) prior to the HRMA's arrival at the XRCF.

2.4.1. Low-Energy Transmission Grating (LETG)

Designed and fabricated by the Space Research Organization of the Netherlands (SRON) and the Max-Planck-Institut für extraterrestrische Physik (MPE), the LETG comprises 540 16-mm-diameter free-standing-gold facets, mounted (3 per module) on a ring structure which locates the facets on the Rowland toroid which includes the focal plane. The Low-Energy Grating (LEG), free-standing gold bars of about 991-nm period, provide high-resolution spectroscopy from 0.08 keV to 2 keV.

Prior to XRCF calibration of the LETG, MPE performed laboratory characterization and calibration of the grating period and period variations at MPE and of transmission efficiency of individual LEG gratings at BESSY. The XRCF activities provided calibration of the ensemble efficiency[16] and the only direct measurement of the line spread function (LSF) and spectral resolution.[17]

2.4.2. High-Energy Transmission Grating (HETG)

Designed and fabricated by the Massachusetts Institute of Technology (MIT), the HETG comprises 336 25-mm-square polyimide-supported-gold facets, mounted (1 per frame) on a ring structure which locates the facets on the Rowland toroid. The HETG functions as 2 gratings with slightly rotated dispersion directions: Medium-Energy Gratings (MEG), with a 400-nm period, lie behind the HRMA's outer 2 mirror shells, for high-resolution spectroscopy from 0.4 keV to 4 keV; High-Energy Gratings (HEG), with a 200-nm period, lie behind the inner 2 shells, for high-resolution spectroscopy from 0.8 keV to 8 keV.

Prior to XRCF calibration of the HETG, MIT performed laboratory characterization and calibration[18,19] of the grating period and period variations at MIT and of transmission efficiency[20,21] of individual MEG and HEG gratings at MIT, NSLS, and BESSY/PTB. The XRCF activities provided calibration of the ensemble efficiency[22] and the only direct measurement of the line spread function(LSF) and spectral resolution.

2.4.3. TMA Objective Grating Assembly (TOGA)

The Massachusetts Institute of Technology (MIT) designed and fabricated the TOGA for use with the TMA (§2.3.2). Employing all 3 flight-type grating facets (LEG, MEG, HEG), oriented with slightly different dispersion directions, the TOGA provided early diagnostic data on each type of grating, as well as the opportunity to rehearse spectroscopy data collection and analysis.

2.5. Focal-plane detectors

The AXAF observatory has 2 focal-plane science instruments — (§2.5.1) the (microchannel plate) High-Resolution Camera (HRC) and (§2.5.2) the AXAF CCD Imaging Spectrometer (ACIS). Each of these instruments provides both an imaging (I) detector and a spectroscopy (S) detector for reading out the dispersed spectra of the LETG or the HETG.

Prior to arrival of the flight detectors (HRC and ACIS) at the XRCF, the rehearsal and the HRMA calibration employed 4 different (non-flight) focal-plane detectors. Of these, 3 detectors — (§2.5.3) an SSD, (§2.5.4) an FPC, and (§2.5.5) the (microchannel plate) High-Speed Imager (HSI) — are part of the HRMA X-ray Detector Assembly (HXDA), which also incorporates a 3-degree-of-freedom stage, an SSD aperture wheel, and an aperture plate for the FPC. The SAO Mission Support Team (MST) provided the HXDA, which, with the (monitor) BNDs (§2.2), comprise the HRMA X-ray Detection System (HXDS). In addition, the (non-flight) ACIS two-chip detector (ACIS-2C) served as a surrogate CCD detector (§2.5.6), to provide practice in CCD data collection and analysis and to calibrate its flight-type CCDs. Ball Aerospace and Technologies designed and fabricated the Five-Axis Mount (FAM) which positioned the ACIS-2C, as well as the 2 flight focal-plane instruments (HRC and ACIS).

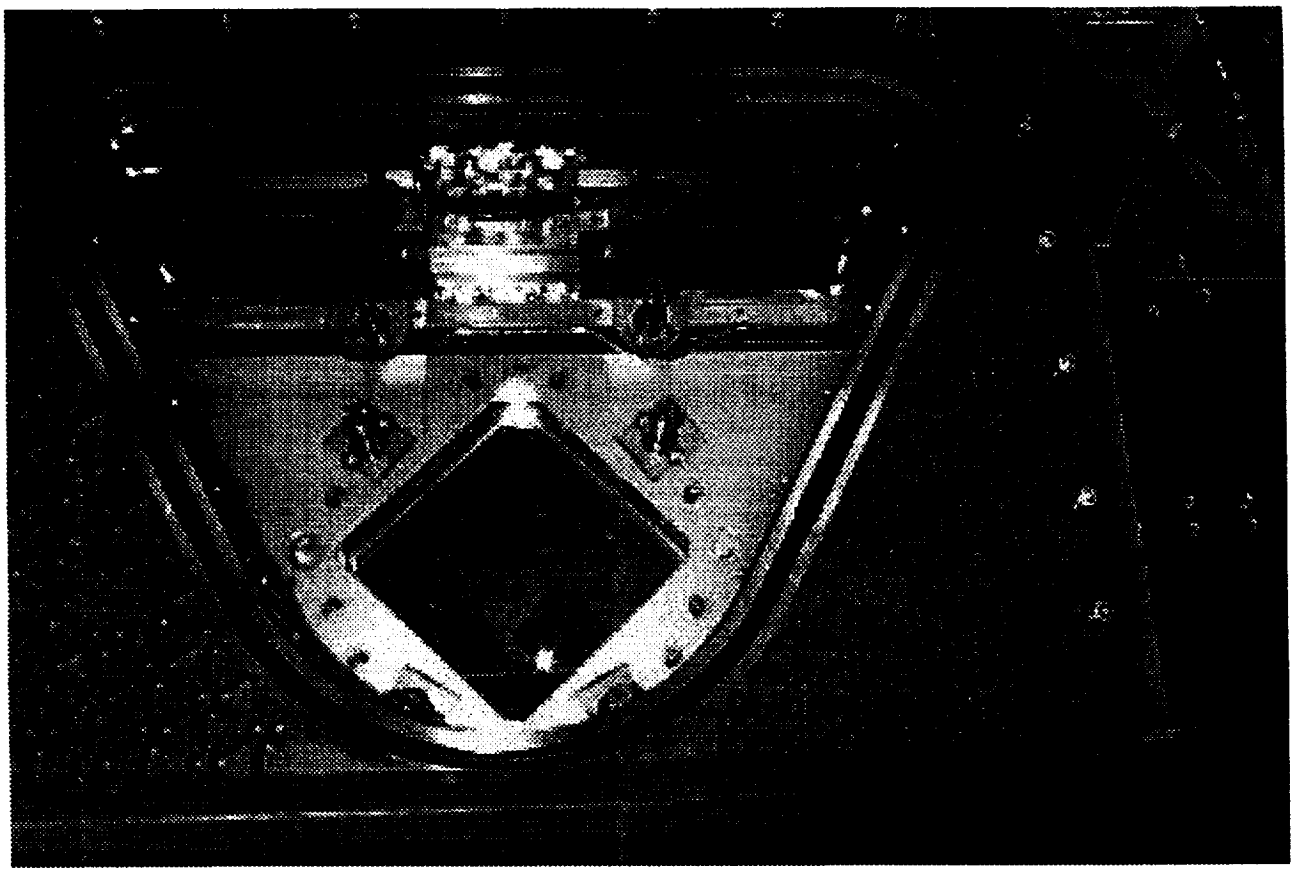

Figure 2. Picture of the High-Resolution Camera (HRC) shows the lay-out of the HRC focal-plane. The imaging detector (HRC-I) is the rotated square at the bottom; the spectroscopy detector (HRC-S), the horizontal strip at the top. An aluminized-polyimide UV/ion shield covers each detector. Just above the top edge of the HRC-S is a reflection filter for optional use to suppress higher-order contributions to LETG spectra. (Photo is from the SAO HRC team.)

2.5.1. High-Resolution Camera (HRC)

The Smithsonian Astrophysical Observatory designed and fabricated the HRC[23] (Fig. 2). The HRC-I (imager) and HRC-S (spectrocopic readout) employ 6-degree-chevron pairs of low-noise microchannel plates (MCPs), coated with cesium–iodide (CsI) and covered with an aluminized-polyimide UV/ion shield. The HRC-I has 10-μm-diameter pores at 12-μm pitch; the HRC-S has 12-μm-diameter pores at 15-μm pitch. The electronic readout employs crossed-grid charge detectors: The HRC-I uses 2 planes of wires; the HRC-I uses wires in the cross-dispersion direction and photo-etched conductors in the dispersion direction. For both HRC-I and HRC-S, the spatial resolution is better than 20 μm ($<$ 0.4 arcsec for the AXAF plate scale) and the readout resolution is 6.4 μm (about 0.13 arcsec). With a 93-mm-square active area, HRC-I has a 31-arcmin-square field of view in the HRMA focal plane; with an approximately 300-mm-by-20-mm area and good soft-x-ray efficiency, the tri-segmented HRC-S is the primary readout for the LETG, providing spectral coverage shortward of 160 Å.

In addition to calibration at the XRCF, the calibration of the HRC[24,25] includes subassembly characterization and calibration of the MCPs, in collaboration with the University of Leicester (UK), including measurements of atomic-edge structure of flight-like CsI-coated MCPs[26] at the Daresbury Synchrotron Radiation Source (UK). In collaboration with the Istituto e Osservatorio Astronomico G. S. Vaiana (Italy), SAO has also characterized the UV/ion shields.[27,28]

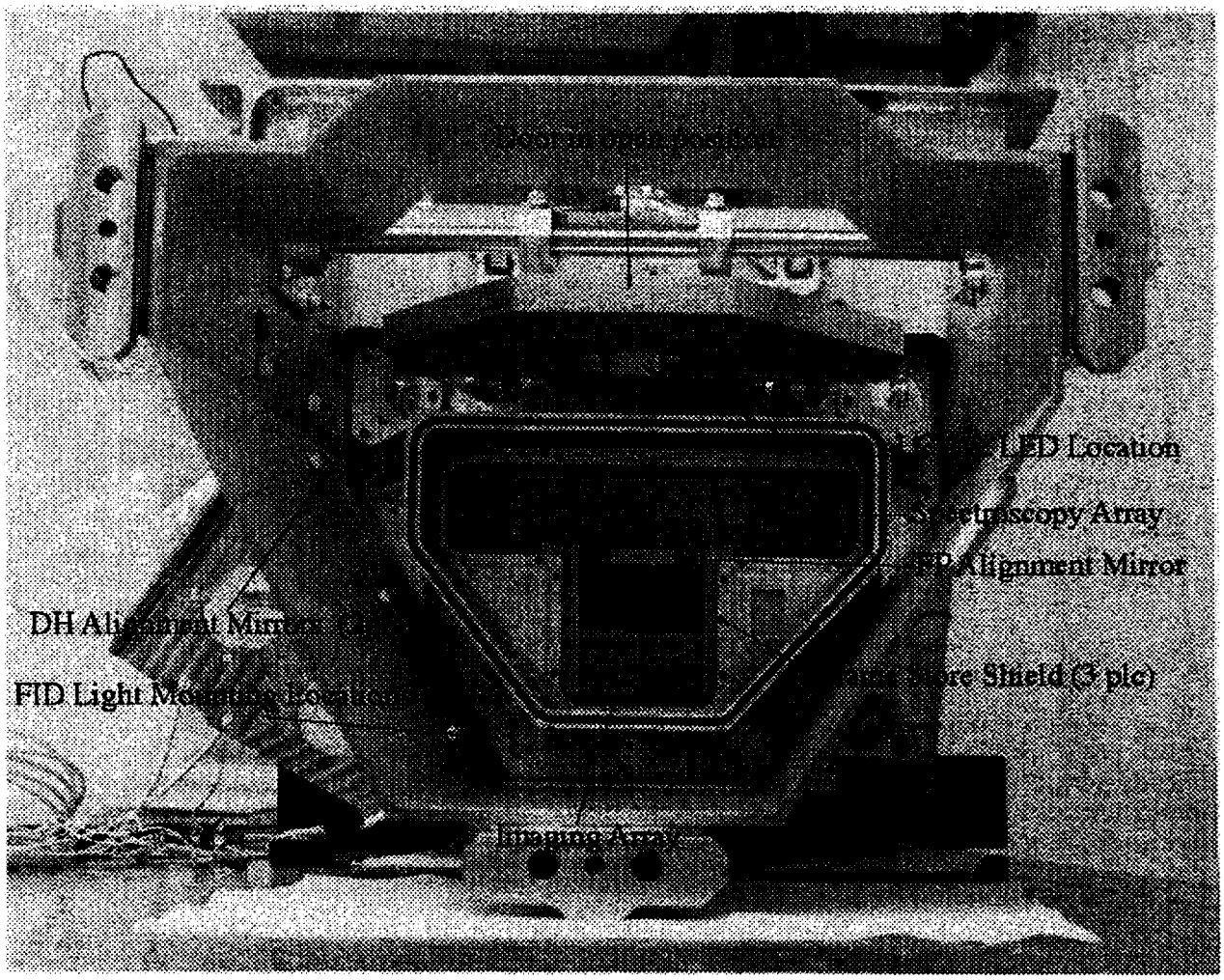

Figure 3. Picture of the AXAF CCD Imaging Spectrometer (ACIS) shows the lay-out of the ACIS focal-plane. The imaging detector (ACIS-I) is the 2-by-2 CCD array at the bottom; the spectroscopy detector (ACIS-S), the 6-by-1 CCD array at the top. Not shown in the picture is the aluminized-polyimide optical blocking shield, which covers both detectors. (Photo is from the MIT ACIS team.)

2.5.2. AXAF CCD Imaging Spectrometer (ACIS)

The Pennsylvania State University (PSU) and the Massachusetts Institute of Technology (MIT) designed and fabricated the ACIS (Fig. 3), with Lockheed–Martin providing some subsystems and integration. The ACIS-I (imager) and ACIS-S (spectrocopic readout) employ large-format (25-mm square) CCDs with 24-μm-square pixels (about 0.5 arcsec for the AXAF plate scale), covered with an aluminized-polyimide optical blocking filter. All the I CCDs and 4 of the 6 S CCDs are front-side devices, with little x-ray response below 0.4 keV; 2 of the S CCDs are back-side, affording useful response down to 0.2 keV. With a 50-mm-square area, ACIS-I has a 17-arcmin-square field of view in the HRMA focal plane. With a 150-mm-by-25-mm area, the ACIS-S is the primary readout for the HETG.

In addition to calibration at the XRCF, the calibration of the ACIS[29] includes subassembly characterization and calibration of the CCD absolute efficiency using atomic-fluorescence sources at MIT[30] and synchrotron measurements at BESSY/PTB, and calibration of the energy scale and spectral resolution using a reflection grating spectrometer — similar to the HIREFS in the XRCF's XSS — at MIT.[31] Pennsylvania State University (PSU) has characterized the optical blocking filters at PSU[32] and, with SAO, at the National Synchrotron Light Source (NSLS).[33]

2.5.3. Focal-plane Solid-State Detector (SSD_X)

One of the 3 detectors of the HRMA X-ray Detector Assembly (HXDA) is a solid-state detector, designated "SSD_X". The SSD_X is identical to the BND (monitor) detector SSD_5 (§2.2.1). Except for the absence of a radioactive calibration source, the SSD_X aperture wheel is also identical to that of SSD_5.

2.5.4. Focal-plane Flow Proportional Counter (FPC_X)

Another of the 3 HXDA detectors is a Flow Proportional Counter, designated "FPC_X". The FPC_X is identical to the 5 BND (monitor) FPCs (§2.2.2). However, a 2-degree-of-freedom aperture plate, with circular apertures up to 36-mm-diameter for measuring encircled energy and slits for measuring dispersed spectra from the OTGs, lies in front of FPC_X.

2.5.5. High-Speed Imager (HSI)

The third HXDA detector is the High-Speed Imager (HSI), an uncoated microchannel plate (MCP), with a 18-mm-diameter active area and readout spatial resolution of 6.4 μm (about 0.13 arcsec for the AXAF plate scale).

2.5.6. ACIS Two-Chip (ACIS-2C)

The ACIS team (PSU and MIT) and SAO designed, fabricated, and operated the ACIS two chip (ACIS-2C), comprised of one front-side CCD and one back-side CCD. Besides providing a surrogate CCD for rehearsing data collection and analysis, the ACIS-2C provided useful data in calibrating the HRMA and HETG, prior to the arrival of the flight ACIS.

3. XRCF CALIBRATION ACTIVITIES

Occurring in about a dozen at-vacuum phases (§3.1), calibration activities at the XRCF Instrument Chamber occupied approximately 6 months of intense (around-the-clock) activity over a one-year period. During this period, calibration of AXAF-observatory (flight) subsystems occupied about 4 months (§3.2), including about 3 x-ray months of remarkably successful data collection. Certainly, the success of the AXAF calibration data collection is due to the dedication and cooperation of the entire AXAF calibration team (§3.3).

3.1. Calibration phases

Table 1. AXAF calibration activities and configurations at the XRCF Instrument Chamber.

CMDB	Phase	X-ray optic	Gratings	FP instrument	Days
	HXDS T&V 1	TMA	TOGA	HXDA	7
A	Rehearsal 1	TMA	TOGA	HXDA	12
B	Rehearsal 2	TMA	TOGA	ACIS-2C	7
	HXDS T&V 2	TMA	TOGA	HXDA	10
C	Calibration 1.1	HRMA	LETG, HETG	HXDA	4
D	Calibration 1.2	HRMA	LETG, HETG	HXDA	26
E	Calibration 1.3	HRMA	LETG, HETG	HXDA	14
F	Calibration 2.1	HRMA	LETG, HETG	ACIS-2C	16
G	Calibration 2.2	HRMA	LETG, HETG	HRC	24
H	Calibration 2.3	HRMA	LETG, HETG	ACIS	8
I	Cross-calibration 1	none	none	ACIS	10
J	Cross-calibration 2	none	none	HXDA	10

Table 1 shows the purpose, configuration, and duration of the approximately dozen AXAF-related phases during which the XRCF Instrument Chamber was at vacuum and x-ray data were being acquired. XRCF calibration of the (flight) AXAF observatory system or subsystems occurred in 6 vacuum phases, which were required for (planned) change-out of focal-plane instrumentation and for (unplanned) repairs to ground-support equipment.

3.2. Observatory calibration timeline

During daily meetings led by Project Science, the Science team planned impending measurements in a detailed Calibration Measurements Data Base (CMDB), maintained by the AXAF Science Center (ASC). Based on the CMDB, the TRW Test Conductor prepared a test-list script for conducting the planned measurements.

Table 2 shows all calibration phases during which the flight optic (HRMA) was present — namely, CMDB prefixes C–H (see Table 1). Recorded in Table 2, for each phase, are the start time of the first measurement, the end time of the last measurement, the duration in x-ray days, the total integration time, the number of measurements, and the average efficiency ((integration days)/(x-ray days)). Despite a few failures in ground-support equipment, which were eventually rectified, daily — and, in some cases, real-time — replanning of the CMDB enabled useful data collection to continue, with minimal loss of efficiency.

Table 2. Timeline for XRCF calibration measurements of the AXAF observatory flight subsystems.

CMDB	First x ray	Last x ray	X-ray days	Integ. days	Measurements	Efficiency
C	12/19/1996 19:35	12/24/1996 05:07	4.40	0.76	96	0.172
D	12/31/1996 13:37	01/26/1997 06:41	25.71	8.07	799	0.314
E	01/28/1997 15:10	02/11/1997 05:11	13.58	6.23	277	0.459
F	02/22/1997 12:11	03/10/1997 23:08	16.46	8.19	584	0.498
G	03/19/1997 16:07	04/12/1997 12:14	23.84	16.31	1111	0.684
H	04/17/1997 23:56	04/26/1997 06:00	8.25	5.50	303	0.666
			92.24	**45.05**	**3170**	**0.488**

3.3. Contributing organizations

Many teams contributed to the success of the AXAF calibration at the XRCF. Here, we briefly summarize the roles of each organization, first those that are primarily engineering (§3.3.1) and then those that are primarily science (§3.3.2). Cooperation among these teams, as well as the individual expertise of each team, were key to this success.

3.3.1. Engineering teams

MSFC Systems Analysis & Integration Laboratory (SAIL) developed and operated the X-Ray Calibration Facility (XRCF), including the X-ray Source System (XSS); managed calibration hardware and configurations; and oversaw repair of ground-support equipment.

TRW Space & Electronics Group coordinated the calibration, serving as Test Conductor; managed flight and ground-support hardware development; and served as the primary interface between engineering and science.

Ball Aerospace & Technologies developed and operated the Five-Axis Mount (FAM) to position the flight focal-plane instruments (HRC and ACIS) and the ACIS-2C.

Eastman Kodak (EKC) developed and operated the HRMA; developed and operated the ground-support actuators for HRMA orientation, OTG insertion, and contamination-cover movement; and developed and operated ground-support HRMA shutters at XRCF.

3.3.2. Science teams

MSFC Project Science (PS) characterized the XSS; coordinated calibration requirements, planning, and execution; oversaw calibration science activities; assisted SAO MST in operating the HXDS; is responsible, with the MST, for analyzing BND data; and is coordinating analysis of the calibration data.

Telescope Scientist (TS) planned, with the MST, the calibration of the HRMA; assisted Project Science in overseeing the calibration science activities; and is responsible, with the MST, for analyzing the HRMA data.

SAO Mission Support Team (MST) developed, calibrated, and operated the HXDS; assisted the ACIS team in developing the ACIS-2C; planned, with the Telescope Scientist (TS), the calibration of the HRMA; is responsible, with the TS, for analyzing the HRMA data; and is responsible for analyzing HXDS (BND and HXDA) data.

AXAF Science Center (ASC) assisted science-instrument teams in planning the calibration; maintained the Calibration Measurements Data Base (CMDB); and ingested all calibration and ancillary data. The ASC Director also assisted Project Science in overseeing the calibration science activities.

SAO HRC team performed and documented HRC subassembly calibration; developed the HRC and operated it at the XRCF; planned XRCF calibration of the HRC; and is responsible for analyzing HRC data.

MIT & PSU ACIS team performed and documented ACIS and ACIS-2C subassembly calibration; developed the ACIS and ACIS-2C and operated them at the XRCF; planned XRCF calibration of the ACIS and ACIS-2C; and is responsible for analyzing ACIS and ACIS-2C data.

MPE & SRON LETG team performed and documented LETG subassembly calibration; developed the LETG; planned XRCF calibration of the LETG; and is responsible for analyzing LETG data.

MIT HETG team performed and documented HETG subassembly calibration; developed the HETG; planned XRCF calibration of the HETG; and is responsible for analyzing HETG data.

4. CALIBRATION RESULTS

Detailed analysis of calibration data is now underway, with a goal of completing most of the analysis approximately 3 months prior to the launch of the AXAF. The calibration of the AXAF observatory occurred in 6 phases with 4 different configurations (§3.1), and comprised nearly 3200 measurements which accumulated nearly 4 million seconds of x-ray data (§3.2). Furthermore, in addition to the focal-plane detector, most measurements involve data for 6 (monitor) BNDs as well as ancillary data (detector settings, apertures, positions, HRMA tilt, source settings, etc.). Owing to the massive body of data to be analyzed and to the ambitious goal of calibrating to an accuracy of a few percent, the calibration analysis promises to be every bit as challenging as the calibration data acquisition. To conclude this overview, we briefly discuss the approach to the calibration analysis (§4.1), describe the types of measurements performed and their objectives (§4.2), and then give 3 examples of key results (§4.3).

4.1. Analysis approach

The purpose of the calibration measurements is, of course, to determine the response of the observatory, for all instrument configurations, to a point source, as a function of x-ray energy, position, and rate. To accomplish this, each science team is developing high-fidelity, physically motivated models. Thus, the objective of the analysis of the calibration data is to determine the model parameters which best fit the entire body of data, modifying the modeled physics where necessary to avoid *ad hoc* empirical adjustments. This approach not only gives a means of interpolating (in energy and position), but also provides a method for transferring the ground-based measurements to an on-orbit calibrated observatory. *In essence, the model is the calibration.*

4.2. Measurement types

For conceptual simplicity, it is customary to decompose the response into spatial and spectral (normalized) redistribution functions and an absolute throughput — i.e., a point (PSF) or line (LSF) spread function, a spectral response matrix, and an effective area. In addition, because a detector's response is nonlinear at sufficiently high rates, owing to pile-up effects, it is necessary to determine the count-rate dependence. Besides, determining the response characteristics for on-axis sources, the calibration also required similar measurements at various off-axis positions.

For the most part, the Calibration Measurements Data Base (CMDB) identified calibration measurements according to the specific characteristic of the response which was the objective of the measurement. In many cases, the measurement's objective also determined the specific technique: For example, small-pinhole (narrow-slit) scans or images measured the core of the PSF (LSF); large-pinhole (wide-slit) wing scans measured the low-surface-brightness scattering wings of the PSF (LSF); non-apertured measurements or defocussed images determined the effective area.

In addition, there were measurements specifically targeted for determining focus, count-rate linearity, spatial linearity, alignment, etc. Many types measurements required data collection at several x-ray energies and off-axis angles.

Figure 4 displays a summed image of all HRC-I and HRC-S x-ray measurements at the XRCF, illustrating the range of measurements comprising the calibration program. Clearly identifiable are the blurry far-off-axis images, the x-shaped sampling pattern of near-axis measurements, the (defocussed ring) OTG effective area measurements, and the concentration of on-axis images.

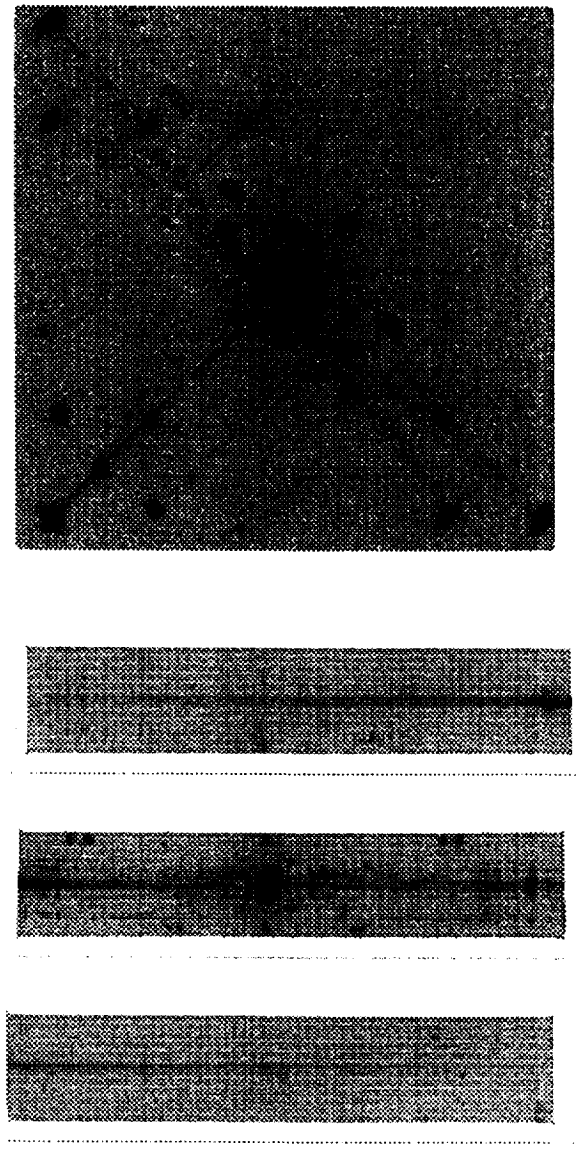

Figure 4. Total accumulated counts in the HRC-I (top) and HRC-S (bottom) indicates the large number and types of measurements performed during the XRCF calibration of the HRC. Note that the displayed HRC-I image should be rotated 45 degrees, such that the mean dispersion direction is horizontal; the 3 displayed HRC-S images should be joined end-to-end. (Images are from the ASC.)

4.3. Examples of key results

As discussed, the calibration team has begun the analysis of the data to determine the physical models and model parameters which, in effect, constitutes the calibration. Several papers presented in these and other† proceedings give many examples of preliminary results. We conclude with 3 sample results, which demonstrate AXAF's unprecedented x-ray capabilities for high-resolution imaging (§4.3.1) and for high-resolution spectroscopy (§4.3.2), but which also indicate the remaining challenge to achieve a few-percent absolute calibration of the effective area (§4.3.3).

4.3.1. Imaging resolution

Figure 5 shows the point spread function of the HRMA–HRC-I, as measured at the XRCF. For the raw data shown, the full width at half maximum (FWHM) is about 0.5 arcsec After correction for "XRCF effects" (HRMA gravitational distortion, finite source size, finite distance), the expected on-orbit FWHM is about 0.3 arcsec. *Clearly, AXAF will provide unprecedented high-resolution imaging for x-ray astronomy.*

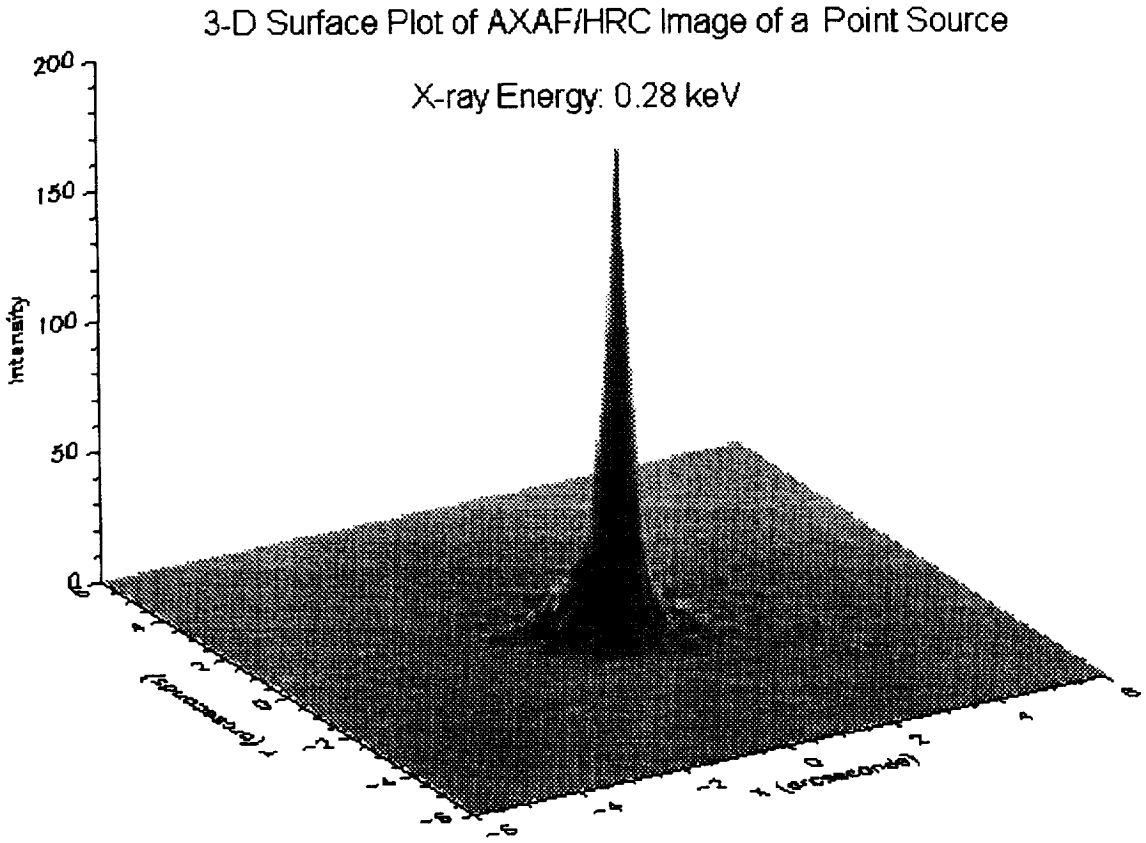

Figure 5. Surface plot of the HRMA–HRC-I point spread function (PSF) at 0.28 keV (C-Kα) shows that the full width at half maximum (FWHM) is about 0.5 arcsec. The expected on-orbit FWHM is about 0.3 arcsec. (Plot is from the SAO HRC team.)

† *EUV, X-Ray, and Gamma-Ray Instrumentation for Astronomy*, O. H. Siegmund and M. A. Gummin, eds., *Proc. SPIE* **3114**, 1997.

4.3.2. Spectroscopic resolution

Figure 6 shows the highly-zoomed, dispersed image of Al-IV (160.07 Å and 161.69 Å) lines from the XSS Penning source (PIGS) for the HRMA–LETG–HRC-S. Analysis of the de-dithered spectrum finds that the LETGS resolving power is at least 1900 near 160 Å — i.e., the LETGS resolution is 0.08 Å. *Clearly, AXAF will provide unprecedented high-resolution spectroscopy for x-ray astronomy.*

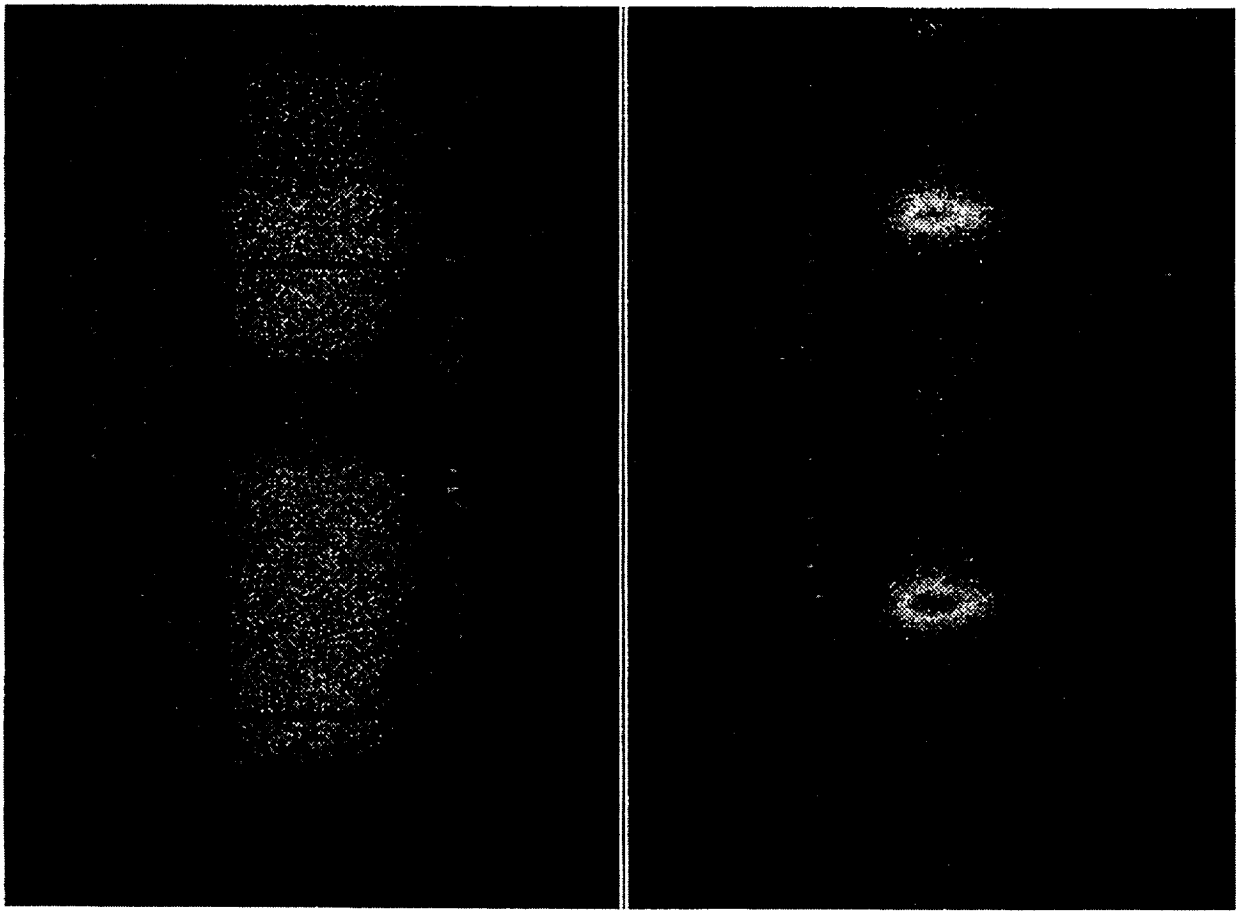

Figure 6. HRMA–LETG–HRC-S highly-zoomed, dispersed image of Al-IV L lines at 160.07 Å (bottom) and 161.69 Å (top) shows that the LETGS resolving power is at least 1900 near 160 Å. Right panel shows the dithered image; left panel, the de-dithered image. Note that the displayed image is not de-gapped and should be rotated 90 degrees, such that the dispersion direction is horizontal. The resolved elongation of the de-dithered image results from the 2-arcsec vertical extent of the Penning-source exit slit. (Images are from the MPE LETG team.)

4.3.3. Effective area

The above 2 examples clearly illustrate the exceptional capabilities of AXAF's optic, gratings, and detectors for high-resolution imaging and high-resolution dispersive spectroscopy. Such calibration measurements are important in confirming the performance predicted on the basis of metrology and simulations and are useful in "calibrating" the point and line spread functions (PSF and LSF). However, the on-orbit PSF and LSF will be what they will be and, in principle, can be measured on orbit. On the other hand, the absolute effective area of the AXAF observatory cannot be determined on orbit; thus, it is essential that this critical property be calibrated accurately on the ground.

Currently, the simulations predict an effective area about 10% higher than that measured at the XRCF.[15] Figure 7 shows this discrepancy for a preliminary determination of the HRMA effective area, based on measurements[34] using

EIPS continuum emission and the SSDs. Other effective-area measurements, using different sources or detectors[15] or with the gratings,[16,22] give similar results — namely, the predicted effective areas generally exceed those measured by about 10%.

One could simply apply an *ad hoc* empirically determined correction, in order to achieve the accuracy goal. However, by understanding the physical mechanism responsible for this discrepancy, we shall not only develop a physical model which accounts for the measured effective area to the desired accuracy but also gain more confidence in the calibration.

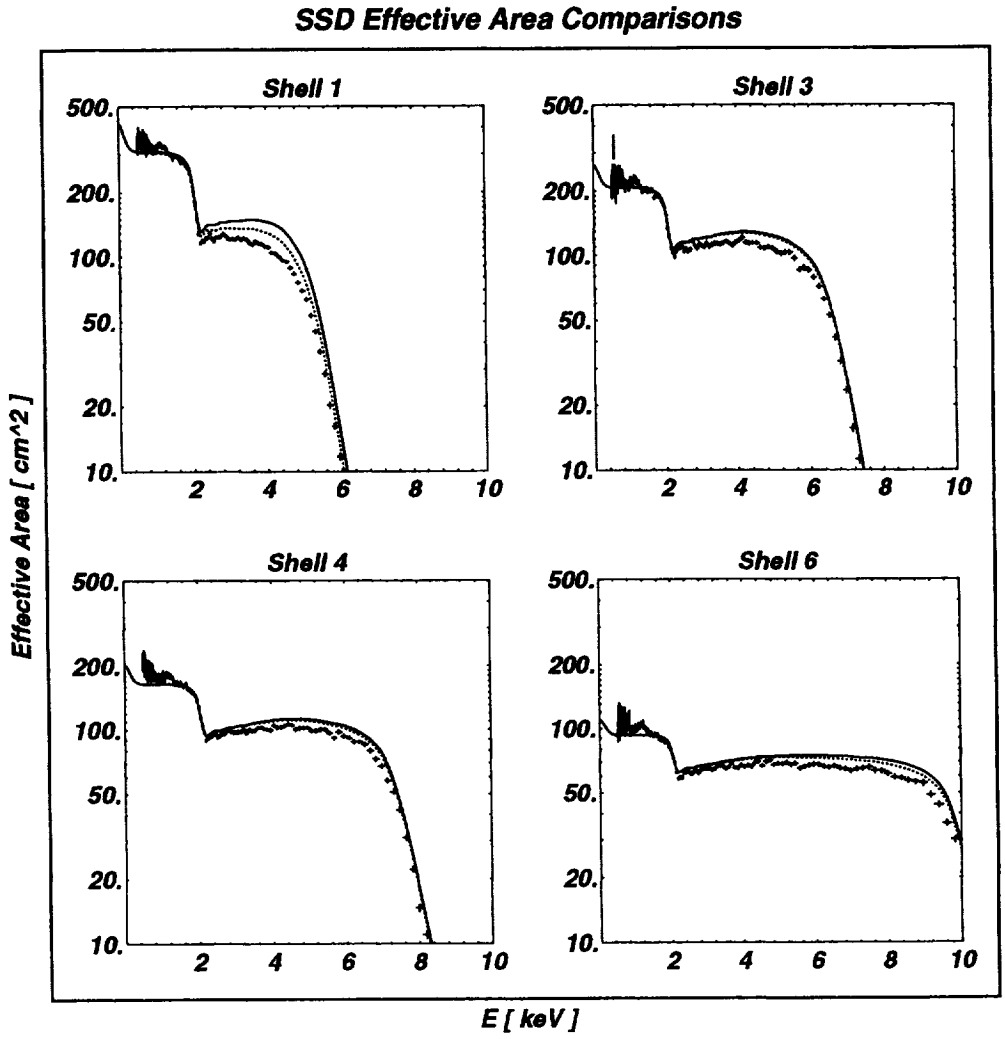

Figure 7. Comparison of the measured with the predicted effective area of each HRMA shell shows a discrepancy of about 10%. The solid line denotes the predicted effective area over the entire focal plane; the dotted line, that within a 2-mm (40-arcsec) diameter. The data points are obtained by dividing the count rate of the focal-plane SSD for a continuum source (EIPS with carbon target at 15 kV) by that of the monitor SSD, and appropriately accounting for distance and aperture. (Plots are from the MSFC Project Science team.)

ACKNOWLEDGEMENTS

Hundreds of individuals, in about a dozen organizations, contributed to the calibration of the AXAF observatory. We gratefully acknowledge their efforts in successfully accomplishing the calibration activities at the XRCF.

APPENDIX A. AXAF-RELATED WEB SITES

The following lists several AXAF-related sites on the World-Wide Web (WWW). Most sites are cross-linked to one another.

`http://asc.harvard.edu/` is the home page of the AXAF Science Center (ASC), operated for NASA by the Smithsonian Astrophysical Observatory (SAO).

`http://wwwastro.msfc.nasa.gov/xray/axafps.html` is the home page of AXAF Project Science, at the NASA Marshall Space Flight Center (MSFC).

`http://hea-www.harvard.edu/HRC/` is the home page of the AXAF High-Resolution Camera (HRC) team, at the Smithsonian Astrophysical Observatory (SAO).

`http://www.astro.psu.edu/xray/axaf/axaf.html` is the home page of the AXAF CCD Imaging Spectrometer (ACIS) team at the Pennsylvania State University (PSU).

`http://acis.mit.edu/` is the home page of the AXAF CCD Imaging Spectrometer (ACIS) team at the Massachusetts Institute of Technology (MIT).

`http://www.rosat.mpe-garching.mpg.de/axaf/` is the home page of the AXAF Low-Energy Transmission Grating (LETG) team at the Max-Planck Institut für extraterrestrische Physik (MPE).

`http://space.mit.edu/HETG/` is the home page of the AXAF High-Energy Transmission Grating (HETG) team, at the Massachusetts Institute of Technology (MIT).

`http://hea-www.harvard.edu/MST/` is the home page of the AXAF Mission Support Team (MST), at the Smithsonian Astrophysical Observatory (SAO).

`http://hea-www.harvard.edu/asctrw/` is the home page of the AXAF X-ray Test Conductors (XTC) from TRW.

`http://elses1.msfc.nasa.gov/xcfdoc/xAhome.html` is the home page of the X-Ray Calibration Facility (XRCF), at the NASA Marshall Space Flight Center (MSFC).

`http://snail.msfc.nasa.gov/sa/axaf/axaf.html` is the AXAF page of the Mission Operations Laboratory at the NASA Marshall Space Flight Center (MSFC).

REFERENCES

1. M. C. Weisskopf, S. L. O'Dell, R. F. Elsner, and L. P. Van Speybroeck, "Advanced X-ray Astrophysics Facility (AXAF): An overview," in *X-Ray and Extreme Ultraviolet Optics*, R. B. Hoover and A. B. Walker, eds., *Proc. SPIE* **2515**, pp. 312–329, 1995.
2. M. C. Weisskopf, S. L. O'Dell, and L. P. Van Speybroeck, "Advanced X-ray Astrophysics Facility (AXAF): An overview," in *Multilayer and Grazing Incidence X-Ray/EUV Optics III*, R. B. Hoover and A. B. Walker, eds., *Proc. SPIE* **2805**, pp. 2–7, 1996.
3. J. Z. Juda, L. P. David, R. H. Donnelly, C. Jones, B. R. McNamara, H. D. Tananbaum, H. L. Marshall, J. P. Hughes, E. M. Kellogg, B. Wargelin, J. H. Chappell, A. Kenter, R. Kraft, S. S. Murray, M. V. Zombeck, M. W. Bautz, J. A. Nousek, D. Dewey, T. H. Markert, A. C. Brinkman, C. J. T. Gunsing, P. Predehl, R. A. Austin, J. J. Kolodziejczak, M. C. Weisskopf, J. W. Arenberg, R. Carlson, and S. C. Texter, "AXAF calibration at the XRCF," *Bull. Am. Astron. Soc.* **187**, p. 7701, 1995.
4. J. J. Kolodziejczak, R. A. Austin, R. F. Elsner, M. K. Joy, M. E. Sulkanen, E. M. Kellogg, and B. J. Wargelin, "X-ray source system at the Marshall Space Flight Center X-Ray Calibration Facility," in *X-Ray and Extreme Ultraviolet Optics*, R. B. Hoover and A. B. Walker, eds., *Proc. SPIE* **2515**, pp. 420–435, 1995.
5. R. F. Elsner, M. K. Joy, S. L. O'Dell, B. D. Ramsey, and M. C. Weisskopf, "Ground-to-orbit transfer of the AXAF-I flux scale: In-situ contamination monitoring of x-ray telescopes," in *Advances in Multilayer and Grazing Incidence X-Ray/EUV/FUV Optics*, R. B. Hoover and A. B. Walker, eds., *Proc. SPIE* **2279**, pp. 332–342, 1994.

6. B. J. Wargelin, J. P. Hughes, E. M. Kellogg, and T. J. Norton, "Ground calibration of AXAF: The HRMA X-ray Detection System (HXDS)," *Bull. Am. Astron. Soc.* **187**, p. 7703, 1995.
7. W. C. McDermott, E. M. Kellogg, B. J. Wargelin, I. N. Evans, S. A. Vitek, E. Y. Tsiang, D. A. Schwartz, R. Edgar, S. Kraft, F. Scholze, R. Thornagel, G. Ulm, M. Weisskopf, S. O'Dell, A. Tennant, J. Kolodziejczak, and G. Zirnstein, "The AXAF HXDS germanium solid-state-detectors," in *EUV, X-Ray, and Gamma-Ray Instrumentation for Astronomy VIII*, O. H. Siegmund and M. A. Gummin, eds., *Proc. SPIE* **3114**, 1997.
8. S. Kraft, F. Scholze, R. Thornagel, G. Ulm, W. C. McDermott, and E. M. Kellogg, "High-accuracy calibration of the HXDS hpGe detector at the PTB radiometry laboratory at BESSY," in *EUV, X-Ray, and Gamma-Ray Instrumentation for Astronomy VIII*, O. H. Siegmund and M. A. Gummin, eds., *Proc. SPIE* **3114**, 1997.
9. L. P. Van Speybroeck, "HRMA performance expectation versus reality," in *Grazing Incidence and Multilayer X-Ray Optical Systems*, R. B. Hoover and A. B. Walker, eds., *Proc. SPIE* **3113**, 1997.
10. D. Jerius, L. Cohen, R. Edgar, M. Freeman, T. Gaetz, J. Hughes, E. M. Kellogg, W. Podgorski, D. Schwartz, L. Van Speybroeck, and P. Zhao, "Predicted x-ray performance of the AXAF high-resolution mirror during ground calibration at the Marshall Space Flight Center," *Bull. Am. Astron. Soc.* **187**, p. 7706, 1995.
11. T. J. Gaetz, R. J. Edgar, M. D. Freeman, W. A. Podgorski, L. P. Van Speybroeck, and P. Zhao, "Focus and alignment of the AXAF optics," in *Grazing Incidence and Multilayer X-Ray Optical Systems*, R. B. Hoover and A. B. Walker, eds., *Proc. SPIE* **3113**, 1997.
12. D. E. Graessle, A. J. Burek, J. J. Fitch, B. Harris, D. A. Schwartz, and R. L. Blake, "Optical constants from synchrotron reflectance measurements of AXAF witness mirrors 2–12 keV," in *Grazing Incidence and Multilayer X-Ray Optical Systems*, R. B. Hoover and A. B. Walker, eds., *Proc. SPIE* **3113**, 1997.
13. J. J. Fitch, A. J. Burek, A. M. Clark, D. E. Graessle, B. Harris, D. A. Schwartz, and R. L. Blake, "AXAF synchrotron witness mirror calibrations 2–12 kev," in *Grazing Incidence and Multilayer X-Ray Optical Systems*, R. B. Hoover and A. B. Walker, eds., *Proc. SPIE* **3113**, 1997.
14. D. E. Graessle, J. J. Fitch, B. Harris, P. Hsieh, D. Nguyen, J. Hughes, D. A. Schwartz, and R. L. Blake, "Calibration of AXAF mirrors using synchrotron radiation," *Bull. Am. Astron. Soc.* **187**, p. 7705, 1995.
15. E. Kellogg, L. Cohen, R. Edgar, I. Evans, M. Freeman, T. Gaetz, D. Jerius, W. C. McDermott, P. McKinnon, S. Murray, W. Podgorski, D. Schwartz, L. Van Speybroeck, B. Wargelin, M. Zombeck, M. Weisskopf, R. Elsner, S. O'Dell, B. Ramsey, A. Tennant, J.Kolodziejczak, G. Garmire, J. Nousek, S. Kraft, F. Scholze, R. Thornagel, G. Ulm, K. Flanagan, D. Dewey, M. Bautz, S. Texter, J. Arenberg, and R. Carlson, "Absolute calibration of the AXAF telescope effective area," in *Grazing Incidence and Multilayer X-Ray Optical Systems*, R. B. Hoover and A. B. Walker, eds., *Proc. SPIE* **3113**, 1997.
16. P. Predehl, H. Bräuninger, A. C. Brinkman, D. Dewey, J. J. Drake, K. A. Flanagan, T. Gunsing, G. D. Hartner, J. Z. Juda, M. Juda, J. Kaastra, H. L. Marshall, and D. Swartz, "X-ray calibration of the AXAF Low-Energy Transmission Grating spectrometer: Effective area," in *Grazing Incidence and Multilayer X-Ray Optical Systems*, R. B. Hoover and A. B. Walker, eds., *Proc. SPIE* **3113**, 1997.
17. A. C. Brinkman, C. J. T. Gunsing, J. S. Kaastra, H. Bräuninger, G. Hartner, P. Predehl, J. J. Drake, J. Z. Juda, M. Juda, D. Dewey, K. A. Flanagan, and H. L. Marshall, "Preliminary test results on spectral resolution of the Low-Energy Transmission Grating spectrometer on board AXAF," in *Grazing Incidence and Multilayer X-Ray Optical Systems*, R. B. Hoover and A. B. Walker, eds., *Proc. SPIE* **3113**, 1997.
18. D. Dewey, D. N. Humphries, G. Y. McLean, and D. A. Moschella, "Laboratory calibration of x-ray transmission diffraction gratings," in *EUV, X-Ray, and Gamma-Ray Instrumentation for Astronomy V*, O. H. Siegmund and J. V. Vallerga, eds., *Proc. SPIE* **2280**, pp. 257–271, 1994.
19. K. A. Flanagan, D. Dewey, and B. Bordzol, "Calibration and characterization of HETG grating elements at the MIT x-ray grating evaluation facility," in *EUV, X-Ray, and Gamma-Ray Instrumentation for Astronomy VI*, O. H. Siegmund and J. V. Vallerga, eds., *Proc. SPIE* **2518**, pp. 438–456, 1995.
20. T. H. Markert, D. Dewey, J. E. Davis, K. A. Flanagan, D. E. Graessle, J. M. Bauer, and C. S. Nelson, "Modeling the diffraction efficiencies of the AXAF high-energy transmission gratings," in *EUV, X-Ray, and Gamma-Ray Instrumentation for Astronomy VI*, O. H. Siegmund and J. V. Vallerga, eds., *Proc. SPIE* **2518**, pp. 424–437, 1995.

21. K. A. Flanagan, T. T. Fang, C. Baluta, J. E. Davis, D. Dewey, T. H. Markert, D. E. Graessle, J. Drake, J. J. Fitch, J. Z. Juda, J. Woo, S. Kraft, P. Bulicke, R. Fliegauf, S. F, G. Ulm, and J. M. Bauer, "Modeling the diffraction efficiencies of the AXAF high-energy transmission gratings: II," in *EUV, X-Ray, and Gamma-Ray Instrumentation for Astronomy VII*, O. H. Siegmund and M. A. Gummin, eds., *Proc. SPIE* **2808**, pp. 650–676, 1996.
22. D. Dewey, K. A. Flanagan, H. L. Marshall, C. Baluta, C. R. Canizares, D. S. Davis, J. E. Davis, T. T. Fang, D. P. Huenemoerder, J. H. Kastner, N. S. Schulz, M. W. Wise, J. J. Drake, J. Z. Juda, M. Juda, A. C. Brinkman, C. J. T. Gunsing, J. S. Kaastra, G. Hartner, and P. Predehl, "Towards the calibration of the HETGS effective area," in *Grazing Incidence and Multilayer X-Ray Optical Systems*, R. B. Hoover and A. B. Walker, eds., *Proc. SPIE* **3113**, 1997.
23. S. S.Murray, J. H. Chappell, A. T. Kenter, K. Kobayashi, R. P. Kraft, G. R. Meehan, M. V. Zombeck, G. W. Fraser, J. F. Pearson, J. E. Lees, A. N. Brunton, S. E. Pearce, M. Barbera, A. Collura, and S. Serio, "AXAF High-Resolution Camera (HRC)," in *EUV, X-Ray, and Gamma-Ray Instrumentation for Astronomy VIII*, O. H. Siegmund and M. A. Gummin, eds., *Proc. SPIE* **3114**, 1997.
24. A. T. Kenter, J. H. Chappell, K. Kobayashi, R. P. Kraft, G. R. Meehan, S. S. Murray, M. V. Zombeck, G. W. Fraser, J. F. Pearson, J. E. Lees, A. N. Brunton, M. Barbera, A. Collura, and S. Serio, "Performance and calibration of the AXAF High-Resolution Camera I: Imaging readout," in *EUV, X-Ray, and Gamma-Ray Instrumentation for Astronomy VIII*, O. H. Siegmund and M. A. Gummin, eds., *Proc. SPIE* **3114**, 1997.
25. R. P. Kraft, J. H. Chappell, A. T. Kenter, K. Kobayashi, G. R. Meehan, S. S. Murray, M. V. Zombeck, G. W. Fraser, J. F. Pearson, J. E. Lees, A. N. Brunton, M. Barbera, A. Collura, and S. Serio, "Performance and calibration of the AXAF High-Resolution Camera II: Spectroscopic detector," in *EUV, X-Ray, and Gamma-Ray Instrumentation for Astronomy VIII*, O. H. Siegmund and M. A. Gummin, eds., *Proc. SPIE* **3114**, 1997.
26. R. P. Kraft, J. H. Chappell, A. T. Kenter, K. Kobayashi, G. R. Meehan, S. S. Murray, M. V. Zombeck, G. W. Fraser, J. F. Pearson, J. E. Lees, A. N. Brunton, M. Barbera, A. Collura, and S. Serio, "Absolute quantum efficiency calibration of the AXAF High-Resolution Camera," in *EUV, X-Ray, and Gamma-Ray Instrumentation for Astronomy VII*, O. H. Siegmund and M. A. Gummin, eds., *Proc. SPIE* **2808**, pp. 194–209, 1996.
27. G. R. Meehan, S. S. Murray, M. V. Zombeck, R. P. Kraft, K. Kobayashi, J. H. Chappell, A. T. Kenter, M. Barbera, A. Collura, and S. Serio, "Calibration of the UV/ion shields for the AXAF High-Resolution Camera," in *EUV, X-Ray, and Gamma-Ray Instrumentation for Astronomy VIII*, O. H. Siegmund and M. A. Gummin, eds., *Proc. SPIE* **3114**, 1997.
28. G. R. Meehan, A. T. Kenter, R. P. Kraft, S. S. Murray, M. V. Zombeck, K. Kobayashi, J. H. Chappell, M. Barbera, and A. Collura, "Measurement of the transmission of the UV/ion shields for the AXAF High-Resolution Camera," in *EUV, X-Ray, and Gamma-Ray Instrumentation for Astronomy VII*, O. H. Siegmund and M. A. Gummin, eds., *Proc. SPIE* **2808**, 1996.
29. M. Bautz, S. Kissel, G. Prigozhin, S. Jones, T. Isobe, H. Manning, M. Pivovaroff, G. Ricker, and J. Woo, "X-ray CCD calibration for the AXAF CCD Imaging Spectrometer," in *EUV, X-Ray, and Gamma-Ray Instrumentation for Astronomy VII*, O. H. Siegmund and M. A. Gummin, eds., *Proc. SPIE* **2808**, pp. 170–181, 1996.
30. H. L. Manning, S. E. Jones, S. E. Kissel, M. W. Bautz, and G. Ricker, "Quantum efficiency calibration of AXAF CCDs from 2 to 10 kev," in *EUV, X-Ray, and Gamma-Ray Instrumentation for Astronomy VII*, O. H. Siegmund and M. A. Gummin, eds., *Proc. SPIE* **2808**, pp. 23–33, 1996.
31. G. Y. Prigozhin, M. W. Bautz, and K. Gendreauand G. R. Ricker, "Calibration of x-ray CCDs with an erect-field grating spectrometer in the 0.2-to-1.5-kev band," in *EUV, X-Ray, and Gamma-Ray Instrumentation for Astronomy VII*, O. H. Siegmund and M. A. Gummin, eds., *Proc. SPIE* **2808**, pp. 260–270, 1996.
32. L. K. Townsley, P. S. Broos, and J. F. Mackay, "Transmission maps of the ACIS UV/optical blocking filter flight units," *Bull. Am. Astron. Soc.* **188**, p. 5501, 1996.
33. G. Chartas, G. Garmire, J. Nousek, D. Graessle, and L. Furenlid, "Measuring the x-ray transmission function of the ACIS UV/optical blocking filters at the National Synchrotron Light Source," *Bull. Am. Astron. Soc.* **188**, p. 5503, 1996.
34. J. J. Kolodziejczak, R. A. Austin, R. F. Elsner, S. L. O'Dell, M. E. Sulkanen, D. A. Swartz, A. F. Tennant, M. C. Weisskopf, G. Zirnstein, and W. C. McDermott, "Uses of continuum radiation in the AXAF calibration," in *Grazing Incidence and Multilayer X-Ray Optical Systems*, R. B. Hoover and A. B. Walker, eds., *Proc. SPIE* **3113**, 1997.